Azimuthal Fourier Coefficients: A simple method to estimate fracture parameters

Jon Downton, Hampson-Russell Software & Services, A CGGVeritas Company, Calgary, Canada
Jon.Downton@CGGVeritas.com
and
Benjamin Roure, Hampson-Russell Software & Services, A CGGVeritas Company, Calgary, Canada

Summary

Azimuthal AVO analysis can be split into two parts: the Amplitude Versus Offset (AVO) analysis and the Amplitude Versus Azimuth (AVAz) analysis. For regularly sampled data in azimuth, the properties of the Fourier transform allow these problems to be treated separately. If we calculate a Fourier transform of the AVAz PP reflectivity data at a particular angle of incidence, we obtain Fourier Coefficients (FCs) that parsimoniously describe the AVAz and anisotropy. It is possible to attach physical significance to each of the FCs by assuming simple rock physics models that relate the anisotropy to the fractures. Assuming a single vertical fracture set, the second FC is approximately equivalent to the anisotropic gradient. Other FCs convey additional independent information about the fractures. The different FCs may be combined in a nonlinear fashion to estimate more fundamental fracture parameters including an unambiguous estimate of the symmetry axis. The FCs are calculated using a limited range of offsets or angles, which places less demands on the data acquisition. This may be advantageous for land 3D data sets, where near offsets are particularly under sampled.

Introduction

Ikelle (1996) and then Sayers and Dean (2001) demonstrated that it is possible to express the azimuthal AVO reflectivity response in terms of a Fourier series as a function of azimuth ϕ. Due to the properties of the Fourier transform, these Fourier coefficients (F.C.'s) represent independent information and may be used in combination or individually to make inferences about the anisotropy and fractures. This work shows how to interpret these F.C.'s in terms of Linear Slip Deformation (LSD) theory (Schoenberg, 1980). Assuming HTI media, with aligned symmetry axes, the physical significance of the individual F.C.'s are described. In particular, the 2nd F.C. corresponds to a biased estimate of the anisotropic gradient. This can be calculated using just one offset or angle of incidence and gives similar results to that obtained by the near offset Rüger equation using multi-offset/angle data. Combinations of F.C.'s may be used to obtain an unbiased estimate of the anisotropic gradient along with an unambiguous estimate of the symmetry axis. In addition, the normal and tangential weakness parameters (Hsu and Schoenberg, 1993) may be individually estimated.

First, the near offset Rüger equation is reviewed with the goal of describing the limitations and parameters calculated as part of an industry standard Azimuthal AVO analysis. Next, Linear Slip Deformation (LSD) theory (Schoenberg, 1980) for HTI media is introduced. This is done to reduce the number of free parameters used to describe the HTI stiffness matrix to make the inversion problem more stable. This has the added benefit of introducing intuitive fracture parameters that describe the azimuthal anisotropy. It is then shown how to relate these parameters to those used in the near offset Rüger equation. Having established these relationships, Fourier transforms and some of their properties are reviewed. The Shaw and Sen (2006) linearized Zoeppritz azimuthal reflectivity, parameterized in terms of linear slip parameters, is then written in the same form as a Fourier series. It

is thus possible to understand the physical significance to each of the F.C.'s. It is then shown that by combining these F.C.'s the normal and tangential weakness parameters may be estimated in a nonlinear fashion. Further, by using both the 2nd and 4th F.C.'s the symmetry axis may be estimated without ambiguity. These techniques are demonstrated with both synthetic and real data.

The near offset Rüger equation

For the case of HTI anisotropy, with the media having the same symmetry axes, the azimuthal reflectivity is described by the Rüger equation (Rüger, 2002). The near offset Rüger equation is

$$R(\phi,\theta) = A + \left(B_{iso} + B_{ani}\cos^2\left(\phi - \phi_{sym}\right)\right)\sin^2\theta, \quad (1)$$

where ϕ represents the source to receiver azimuth, θ is the average angle of incidence, A is the intercept, B_{iso} is the isotropic gradient, B_{ani} is the anisotropic gradient and ϕ_{sym} is the azimuth of the symmetry axis. Hudson (1981) theory may be used to show that the anisotropic gradient B_{ani} is proportional to the crack density. The symmetry axis is perpendicular to the strike of the fractures. This near offset approximation ignores higher angle terms, introducing a bias into the B_{ani} estimate. The advantage of using this approximation is that equation (1) may be linearized by rewriting it in terms of $cos(2\phi)$ and $sin(2\phi)$ and thus be solved in a straightforward fashion using least squares inversion (Downton and Gray, 2006). The disadvantage of this approximation is that it is impossible to tell whether the anisotropic gradient is positive or negative, thus introducing a 90 degree ambiguity into the estimate of ϕ_{sym}.

Linear slip theory

The LSD theory (Schoenberg, 1980) allows fractures to be modeled as a perturbation of the background compliance of the unfractured rock. The total compliance of the rock **S** is the sum of the background compliance $\mathbf{S}_b$ plus the compliance due to the fractures $\mathbf{S}_f$. The fractures can be modeled as an imperfectly bonded interface where the traction is continuous but the displacement might be discontinuous. The displacement discontinuity is linearly related to the traction and in its simplest form, the fractures normal to the x-axis, gives rise to HTI anisotropy (Schoenberg and Sayers, 1995). For example, the displacement discontinuity normal to the fracture is proportional to the normal stress. This proportionality constant is the normal fracture compliance B_N. Similarly, the tangential fracture compliance B_T may be defined. Instead of working with compliances, I choose to parameterize the problem in terms of the normal weakness parameter $\delta_N = MB_N./(1+MB_N)$, and tangential weakness parameter $\delta_T = \mu B_T./(1+\mu B_T)$, where $M=\lambda+2\mu$. These are fractional parameters which range from 0 to 1. In both cases when the fracture weakness is zero the fracture has no influence on the compliance. Bakulin (2000) shows that the anisotropic gradient may be written in terms of these weakness parameters so that $B_{ani}=g(\delta_T - \chi\delta_N)$ where $\chi=1-2g$ and g is the square of the S-wave to P-wave velocity ratio of the unfractured rock. The difference operator Δ represents the difference in layer properties between the lower and upper media, thus $\Delta\delta_T$ is the difference in tangential weakness between the two layers. For future reference the variable $\kappa=g(\delta_T - g\delta_N)$ is also introduced. Both κ and B_{ani} are weighted differences of the tangential and normal weaknesses with slightly different weighting factors.

Fourier series

The discrete Fourier series for a periodic discrete function $R(\phi)$ over the interval (-π, π) is

$$R(\phi,\theta) = \sum_{n=0}^{\infty}\left(u_n(\theta)\cos(n\phi) + v_n(\theta)\sin(n\phi)\right). \quad (2)$$

The discrete Fourier coefficients can be calculated by taking the dot product of $R(\theta,\phi)$ for a particular angle of incidence with either a cosine series

$$u_n(\theta)=\frac{1}{\pi}\sum_{k=1}^{N}R_k(\phi,\theta)\cos(n\phi)\,d\phi, \tag{3}$$

or a sine series

$$v_n(\theta)=\frac{1}{\pi}\sum_{k=1}^{N}R_k(\phi,\theta)\sin(n\phi)\,d\phi, \tag{4}$$

for integer values of n such that $n \geq 0$. Alternatively, the Fourier series can be written in terms of the magnitude

$$r_n(\theta)=\sqrt{u_n^2(\theta)+v_n^2(\theta)}, \tag{5}$$

and phase

$$\phi_n(\theta)=\frac{1}{n}\arctan\left(\frac{v_n(\theta)}{u_n(\theta)}\right). \tag{6}$$

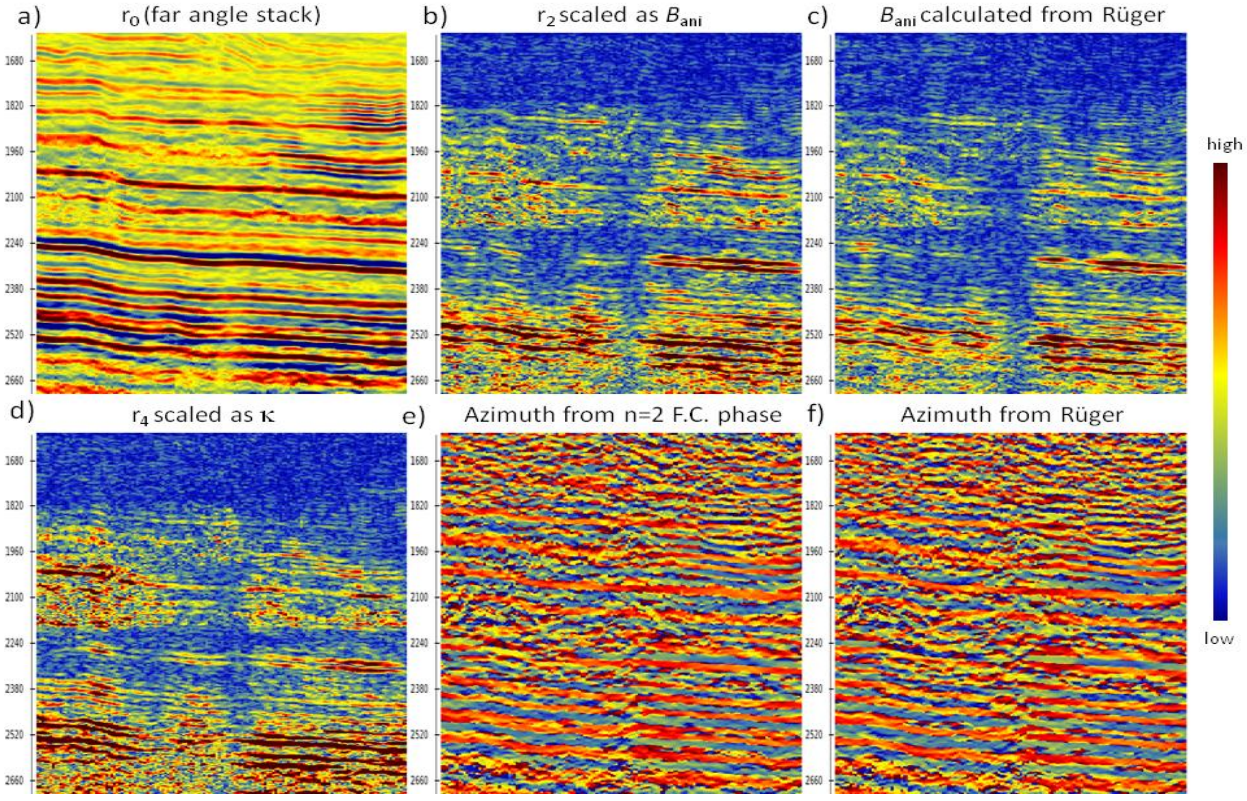

Figure 1: A crossline from a Canadian 3D showing the FCs compared to the anisotropic gradient (c) and isotropy plane azimuth (f) obtained from the near offset Rüger equation. The Fourier coefficients were calculated on azimuth sectored stacks with an average incidence angle of 35 degrees. The n=0 FC (a) is equivalent to the average 35 degree angle stack. The scaled n=2 FC (b) closely matches the anisotropic gradient (c) from the near offset Rüger equation. The scaled n=4 FC (d) or κ contains independent information from the n=2 FC (b) but also has many similarities. The azimuth calculated from the n=2 FC phase (e) matches closely to that obtained from the Rüger equation (f).

Thus

$$R(\phi,\theta) = r_0 + \sum_{n=1}^{\infty} r_n(\theta)\cos\left(n(\phi - \phi_n(\theta))\right). \quad (7)$$

Because of reciprocity P-wave seismic data only has even values of n. The D.C. component (n = 0) is equivalent to the average angle stack. Figures 1a, 1b and 1d display for a particular crossline the magnitude for the n = 0, 2, and 4 F.C.'s calculated at an average angle of incidence of 35 degrees for a 3D seismic dataset from Western Canada.

Azimuthal reflectivity

Shaw and Sen (2006) derived an azimuthal reflectivity expression for aligned HTI media parameterized in terms of normal and tangential weaknesses. Writing this expression in terms of F.C.'s results in

$$R_{pp}(\phi,\theta) = r_0(\theta) + r_2(\theta)\cos\left(2(\phi - \phi_{sym})\right) + r_4(\theta)\cos\left(4(\phi - \phi_{sym})\right), \quad (8)$$

where

$$r_0(\theta) = A + B\sin^2\theta + C\sin^2\theta\tan^2\theta, \quad (9)$$

$$r_2(\theta) = \frac{1}{2}\left(B_{ani} + g(g-1)\Delta\delta_N\tan^2\theta\right)\sin^2\theta, \quad (10)$$

and

$$r_4(\theta) = \frac{1}{8}\kappa\sin^2\theta\tan^2\theta. \quad (11)$$

The D.C. component (n = 0) is equivalent to the classic 3-term AVO expression. In this case, the coefficients A, B and C are also a function of the normal and tangential weaknesses. For small angles of incidence, the n = 2 F.C. is approximately $r_2(\theta) \approx 0.5 * B_{ani}\sin^2\theta$ thus the anisotropic gradient is just a scaled version of the second Fourier coefficient. For example, at an angle of 30.0°, B_{ani} =8*|r_2|. This is a biased estimate of the anisotropic gradient since the $\sin^2\theta\tan^2\theta$ term is ignored. However, it has similar accuracy to the near offset Rüger equation since the same order term is also ignored. Figures 1c and 1b compare the anisotropic gradient obtained using the near offset Rüger equation with that obtained using a single F.C. for n=2 at a single angle of incidence. The symmetry axis is calculated from the n=2 F.C. phase using equation (6). It is important to note that in calculating the magnitude the positive root is used. Thus, similar to the Rüger equation, when B_{ani} is actually negative, the estimated azimuth needs to be rotated 90°. Figures 1e and 1f show the close match between isotropy plane azimuths obtained by the two methods. The n = 4 F.C. is just a scaled version of the variable κ (Figure 1d). For arbitrary anisotropic symmetries (Ikelle, 1996) the largest coefficient for the linearized version of the Zoeppritz equation is n = 4.

Nonlinear inversion

The parameters B_{ani} and κ are both linear combinations of $\Delta\delta_N$ and $\Delta\delta_T$, thus it should be possible to independently solve for these parameters. In practice this is complicated due to the fact that the F.C.'s are estimating magnitudes rather than signed values of these quantities (i.e. | B_{ani} | and |κ |). In order to determine the signed values, the symmetry axis must be determined. This problem is nonlinear but can be determined using multiple angles of incidence and the n = 2 and n = 4 F.C.'s.

Figure 2 shows the results of a nonlinear inversion on synthetic data. Being a nonlinear problem the misfit function is multi-modal. In order to verify that the nonlinear inversion correctly estimates the global misfit minimum, a large number of models were tested (> 16,000). Different combinations of the

symmetry axis, normal and tangential weaknesses were used to generate forward models using the Zoeppritz equation. Noise was added to create a signal-to-noise ratio of 10:1. The resulting synthetic data were then inverted for the isotropy plane ϕ_{iso}, $\Delta\delta_N$ and $\Delta\delta_T$. B_{ani} and κ were also calculated from $\Delta\delta_N$ and $\Delta\delta_T$. Figure 2 shows the estimated variables compared to the actual variables. If the estimated value corresponds to the ideal value the points should be on the diagonal line connecting the lower hand left corner to the upper right hand corner. The figures are color coded so that the color represents the number of solutions that fall within a particular bin. The nonlinear inversion properly assigns the correct sign to B_{ani} in 99.5% of the models (Figure 2b). In the case when $\kappa = 0$ (a small percentage of the models) the n = 4 F.C. is non-informative and there is not enough information to uniquely determine the symmetry axis. This contrasts with the near offset Rüger equation (Figure 2a) where only positive values of B_{ani} are estimated. Further, the small B_{ani} values estimated by the Rüger equation show significant bias due to the neglection of the higher offset term. There is little error in the azimuthal estimate other than the points associated with $\kappa = 0$. The normal and tangential weakness estimates plot along the diagonal again showing the estimated values accurately predict the majority of cases. Only the normal weakness is shown in Figure 2c due to lack of space, but the tangential weakness behaves in a similar fashion. There is slightly more dispersion in the estimates of $\Delta\delta_N$ and $\Delta\delta_T$ than B_{ani} and κ due to the magnification of the noise through the reparameterization.

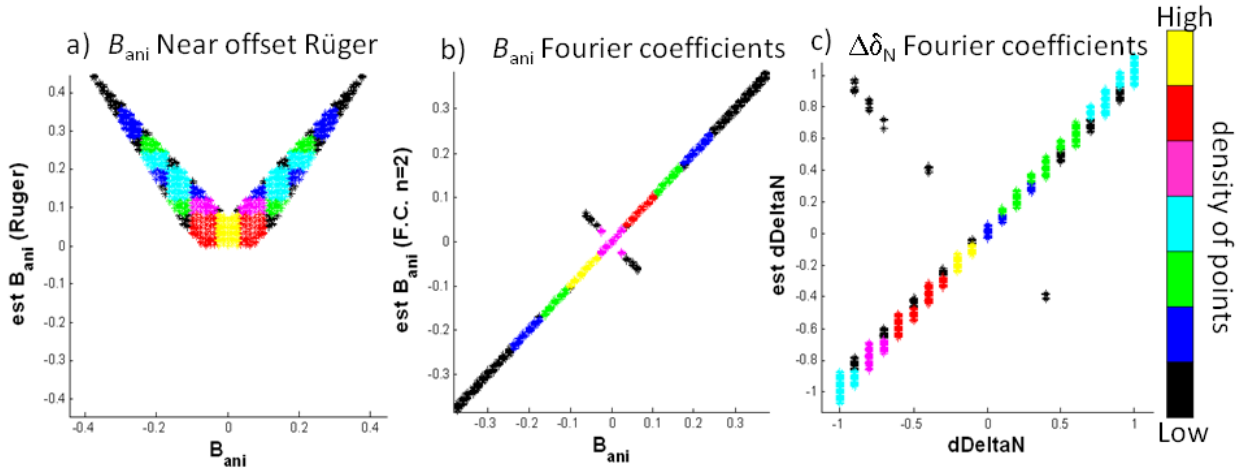

Figure 2: Comparison of estimated versus actual model parameters. If the estimate matches the actual value it should fall along the main diagonal. The colors represent how many estimates fall within a particular bin. Figure 2a shows this for the anisotropic gradient calculated using the near offset Rüger equation while 2b shows the anisotropic gradient calculated using the nonlinear inversion using Fourier coefficients. Figure 2c) shows the estimated versus actual normal weaknesses $\Delta\delta_N$. It is slightly more sensitive to noise.

Figure 3 illustrates the results of this nonlinear inversion on a dataset from Western Canada. Figure 3a shows the Anisotropic Gradient calculated from the magnitude of the 2nd FC of one particular incidence angle. Similar to the Rüger result, all the B_{ani} values are positive. Since the sign of B_{ani} is not available this introduces a 90 degree ambiguity into the azimuth estimate (Figure 3c) which shows up as a layering effect in the display. The nonlinear inversion resolves the sign ambiguity of B_{ani} (Figure 3b) also changing the amplitudes slightly because of the more accurate theoretical model. Recall, the near offset Rüger (and linear) inversion ignores the far offset term introducing a bias for small values of B_{ani} (Figure 2a and 2b). The nonlinear azimuth estimate (Figure 3d) has a much more stable azimuth direction consistent with the dominant stress regime of 135 degrees. This behavior is more geologically believable.

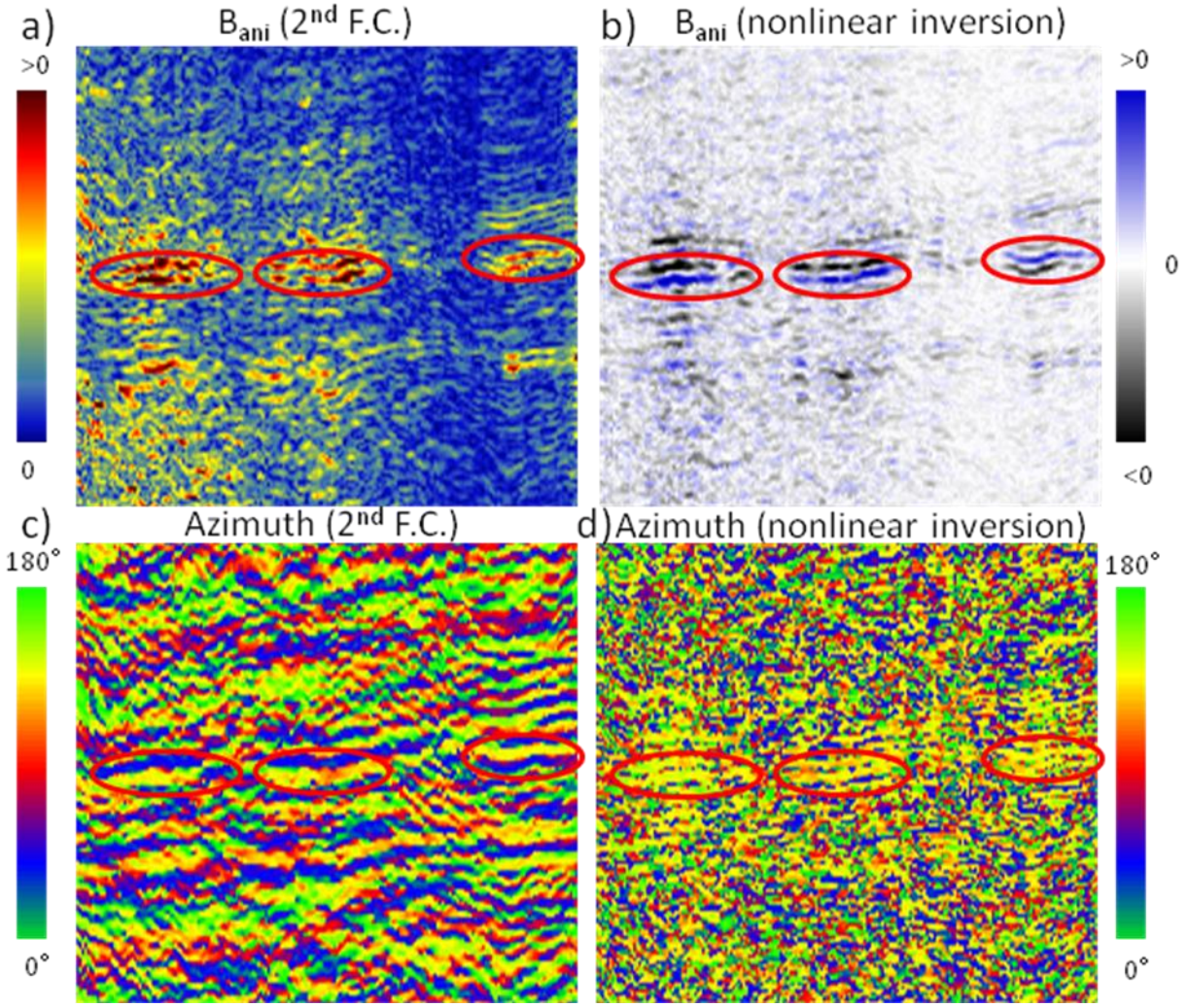

Figure 3: A crossline from a Canadian 3D showing B_{ani} calculated from a single FC (a) compared to the anisotropic gradient estimate from multiple FCs input into a nonlinear inversion (b). The nonlinear B_{ani} has both positive and negative values. The azimuth calculated from the nonlinear inversion (d) is consistent with the dominant stress in the area (135 degrees) and does not show the same periodicity as the azimuth calculated in a linear fashion similar to the Rüger equation.

Conclusions

The use of azimuthal Fourier coefficients allows one to decouple the azimuthal AVO analysis into two parts; the traditional AVO analysis and an azimuthal amplitude analysis. The fracture parameters primarily influence the azimuthal amplitude response and can be isolated by observing non-zero F.C.'s. The n=0 F.C. has the same form as the traditional three-term AVO problem and may be solved in a traditional fashion. In the case of aligned HTI media described by linear slip theory, the results of the two analyses can be combined to uniquely determine (in the majority of cases) the symmetry axis, the fractional P-wave velocity, S-wave velocity, density, normal and tangential weaknesses or variations thereof.

The parameters typically determined by the near offset Rüger equation, the anisotropic gradient and the symmetry axis, can be obtained using just the 2nd F.C. calculated on one angle stack. The uncertainty of these estimates decrease as the angle of incidence is increased. By using additional F.C's and angles of incidence, the symmetry axis ambiguity can be resolved and an improved estimate of the anisotropic gradient obtained. This additional analysis relies on information from the 4th F.C. which is typically noisier than the 2nd F.C. Both these F.C.'s can be quality controlled to determine their

reliability. Even though they both provide independent information, both are weighted sums of the normal and tangential weaknesses and should be correlated.

Acknowledgements

The authors thank EnCana and Apache for permission to show this data. We thank Didier Lecerf of CGGVeritas for discussions that lead to this research, Bill Goodway and Marco Perez for motivating us to move beyond the Anisotropic Gradient. We thank Lee Hunt and Fairborne for feedback they gave us while developing these attributes. In addition we thank Darren Schmidt, Alicia Veronesi, Dan Hampson and Brian Russell of Hampson-Russell for support they gave in creating this work.

References

Bakulin, A., V. Grechka, and I. Tsvankin, 2000, Estimation of fracture parameters from reflection seismic data—Part I: HTI model due to a single fracture set, Geophysics, 65, 1788

Downton, J., and D. Gray, 2006, *AVAZ parameter uncertainty estimation;* SEG Expanded Abstracts, 25,234

Hsu, J.C., and M. Schoenberg, 1993, Elastic waves through a simulated fractured medium, Geophysics,58,964

Ikelle L.T. 1996. Amplitude variations with azimuths (AVAZ) inversion based on linearized inversion of common azimuth sections. In: Seismic Anisotropy (eds E. Fjaer, R. Holt and J.S. Rathore), pp. 601±644. SEG, Tulsa.

Hudson, J. A., 1981, Wave speeds and attenuation of elastic waves in material containing cracks, Geophys. J. Royal Astronomy. Soc. 64, 133-150.

Rüger, A., 2002, Reflection coefficients and azimuthal AVO Analysis in anisotropic media, SEG geophysical monograph series number 10: Soc. Expl. Geophys.

Sayers, C., and S. Dean, 2001, Azimuth-dependent AVO in reservoirs containing non-orthogonal

fracture sets: Geophysical Prospecting, 2001, 49, 100-106.

Schoenberg., M., 1980, Elastic behaviour across linear slip interfaces. Journal of the Acoustical Society of America, 68:1516–1521

Schoenberg, M., and C. Sayers, 1995, Seismic anisotropy of fractured rock, Geophysics, **60**, 204–211.

Shaw, R.K., and M. K. Sen, 2006, Use of AVOA data to estimate fluid indicator in a vertically fractured medium, Geophysics,71,C15